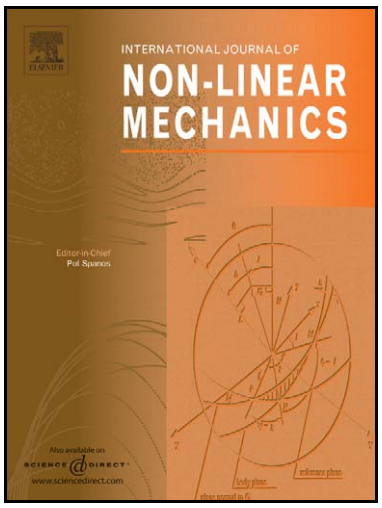

www.elsevier.com/locate/nlm

On the modelling of highly elastic flows of amorphous thermoplastics

Łukasz Figiel, C. Paul Buckley

PII: S0020-7462(09)00015-8
DOI: doi:10.1016/j.ijnonlinmec.2009.01.005
Reference: NLM 1577

To appear in: *International Journal of Non-Linear Mechanics*

Received date: 23 September 2008
Revised date: 19 January 2009
Accepted date: 20 January 2009

Cite this article as: Łukasz Figiel and C. Paul Buckley, On the modelling of highly elastic flows of amorphous thermoplastics, *International Journal of Non-Linear Mechanics* (2009), doi:10.1016/j.ijnonlinmec.2009.01.005

On the modelling of highly elastic flows of amorphous thermoplastics

Łukasz Figiel* **and C. Paul Buckley**
Department of Engineering Science, University of Oxford, Parks Road, OX1 3PJ, UK

Abstract
Two approaches to the kinematic structuring of constitutive models for highly elastic flows of polymer melts have been examined systematically, assuming either: (1) additivity of elastic and viscous velocity gradients, or (2) multiplicability of elastic and viscous deformation gradients. A series of constitutive models was compared, with differing kinematic structure but the same linear responses in elastic and viscous limits. They were solved numerically and their predictions compared, and they were also compared to those of the Giesekus model. Several variants, previously proposed as separate models, are shown to be equivalent and qualitatively in agreement with experiment, and therefore a sound basis for construction of models. But the assignment of viscous spin is critical: if it is assumed equal to the total spin with approach (1), or equal to zero with approach (2), then unphysical viscoelastic behaviour is predicted.

Keywords: viscoelastic flow; thermoplastic polymers, constitutive model; finite strain.

1. Introduction

Industrial forming processes for thermoplastic polymers frequently involve large deformations in a time/temperature range where flow is highly elastic. Physically, this arises from the great lengths of the molecules. All molecules with molar mass M larger than a monomer-specific critical value M_e, are topologically constrained by their neighbours, linking them into a continuous molecular network even in the molten state – that is, when they are amorphous and above the glass transition temperature T_g. Connectivity is provided by molecular entanglements. Such a network has an elastic, rubber-like, constitutive response when unrelaxed. It can relax fully, but only by the

* Corresponding author. Tel.: +44 1865 283487; fax: +44 1865 273 906. E-mail address: Lukasz.Figiel@eng.ox.ac.uk (Ł. Figiel).

tortuous process of molecular disengagement that has come to be known as "reptation", with an associated relaxation time τ_d. Industrial polymers usually have $M>>M_e$, and $\tau_d \propto (M \div M_e)^\beta$ where $\beta \sim 3.4$ (Ferry, 1980), so relaxation times are exceptionally long compared to other viscoelastic liquids. Moreover, economic necessity requires industrial forming processes for polymers to be as rapid as possible. Consequently polymers are frequently melt-processed on time scales not far below τ_d.

In such flows, elastic stretch of the entanglement network is only partially relaxed. This is especially true of processes such as stretch-blow moulding and thermoforming of sheets where substantial elasticity of the melt is advantageous to stability of the process. Network stretch, and hence mutual alignment of the molecules, is also an essential requirement for stress-induced crystallisation (e.g. during blow-moulding of polyester bottles or spinning of polyamide fibres). Moreover, the complexity of nonlinear viscoelastic material behaviour is often combined with large-scale geometrical nonlinearity. An example of this is the finite rotation encountered when the flow has a large shear component, for example around rigid particles in modelling of the forming of particulate-reinforced polymers.

This paper is motivated by the engineering need to model highly elastic polymer flows, in a manner suitable for optimisation in the context of numerical simulation of polymer processes. Clearly, numerical modelling of such processes requires a constitutive model that is robust under arbitrarily large deformations and in the presence of a high degree of elasticity. The question of how best to achieve this remains a matter of dispute. A particular difficulty is that solutions have been proposed in two different branches of the literature – solid mechanics and fluid mechanics – and hence it has been unclear how they are all related. The present note aims to clarify the issues, and assist the development of suitable constitutive models, by comparing systematically the kinematic assumptions embedded in various approaches, and highlighting how they are related.

Previous authors attempting to capture accurately, but empirically, highly elastic flows of amorphous polymers have adopted a range of strategies. Some have ignored the problem altogether and have approximated the polymer response as wholly viscous (G'Sell and Jonas, 1979; Chevalier and Marco, 2007) or wholly elastic but with rate and temperature-dependent parameters (Sweeney et al. 1995; Matthews et al. 1997). While it

is possible to fit experimental data for a given monotonic strain sequence in this way, it is clearly impossible to capture an arbitrary deformation history with such approaches. Other authors proposing finite deformation viscoelastic models, in view of the lack of experimental evidence for how the antisymmetric part of the velocity gradient (i.e. the spin) should be apportioned between viscous flow and elastic deformation, have cautiously declined to speculate on this point and their proposed models are incomplete in this respect (Vigny et al. 1999; Adams et al. 2000; Dooling et al. 2002; Makradi et al. 2005).

Those authors that have proposed complete three-dimensional models have adopted one of three approaches. One group have employed models based on additive split of the rate of deformation tensor (Nemat-Nasser, 1979, 1982) together with the assumption of zero viscous spin (Leonov, 1976). Another group assumed multiplicative decomposition of the deformation gradient (Kröner, 1960; Lee, 1969), together with a particular, convected, interpretation of the viscous velocity gradient and the assumption of zero viscous spin (Boyce et al. 2000; Dupaix and Boyce, 2007; Drozdov et al. 2008). Finally, several authors have employed models expressed in terms of convected derivatives of stress, such as the upper convected Maxwell model (UCM), see for example Poitou et al. (2003), or the more robust Giesekus modified UCM or a finite extensibility adaptation of it (Doufas et al. 2000). In addition, the literature provides a number of physically based models with similar structure, that quite successfully capture polymer melt viscoelasticity under a wide range of conditions. An attractive feature of these is that they embody awareness of molecular architecture. Examples are the Pom-Pom model (McLeish and Larson, 1998) for branched molecules and the Rolie-Poly model (Likhtman and Graham, 2003) for linear molecules. However these do not yet capture accurately the highly elastic extensional flows of interest here, without empirical extensions. For authoritative reviews of polymer melt constitutive models to date, and their links to molecular structure, the reader is referred to Larson (1988) and Dealy and Larson (2006).

The present paper considers classes of constitutive models that may be conveniently fitted to experimental data under relevant conditions. These models are kinematically structured a priori to capture naturally the geometrical nonlinearity, before

insertion of a description of the physical response, that may be either empirical or physically-inspired. Two approaches to their kinematic structure are compared in this work: (1) approach I is based on additive decomposition of the velocity gradient tensor, while (2) approach II is based on multiplicative decomposition of the deformation gradient tensor. In order to highlight the consequences of purely *geometric* non-linearity arising from different kinematic assumptions made, models considered here based on each approach are *linear* in both the elastic and viscous limits. Thus elastic response is taken to be neo-Hookean, while viscous response is taken to be Newtonian.

The Giesekus model provides a convenient bench-mark, as its variable parameter α ($0 \le \alpha \le 1$) allows several models to be recovered from a single equation.

2. Approaches

Consistent with the aim of modelling highly elastic flows where stresses may be sufficient for detectable volume change to occur, in the models considered here there is a reversible volumetric contribution to the deformation gradient. Thus we begin with a multiplicative decomposition of the deformation gradient $\boldsymbol{F}$ into its volumetric ($\boldsymbol{F}_{\text{vol}}$) and isochoric ($\hat{\boldsymbol{F}}$) parts (Flory, 1961)

$$\boldsymbol{F} = \boldsymbol{F}_{\text{vol}}\hat{\boldsymbol{F}}, \text{ where } \hat{\boldsymbol{F}} = J^{-\frac{1}{3}}\boldsymbol{F}, \text{ and } J = \det \boldsymbol{F}. \tag{1}$$

J is the volume ratio. The viscoelastic response is then all contained within the isochoric part of the velocity gradient $\hat{\boldsymbol{F}}$. Its corresponding left Cauchy-Green tensor and velocity gradient, and the latter's symmetric (deformation rate) and skew-symmetric (spin) parts are defined by

$$\hat{\boldsymbol{B}} = \hat{\boldsymbol{F}}\hat{\boldsymbol{F}}^{\mathrm{T}}; \ \hat{\boldsymbol{L}} = \dot{\hat{\boldsymbol{F}}}\,\hat{\boldsymbol{F}}^{-1}, \text{ and } \hat{\boldsymbol{D}} = \operatorname{sym}\left[\hat{\boldsymbol{L}}\right], \text{ and } \hat{\boldsymbol{W}} = \operatorname{skew}\left[\hat{\boldsymbol{L}}\right]. \tag{2}$$

In order to avoid unnecessary complexity, we now restrict attention to only those materials whose response to volume change is purely elastic (a good approximation in the case of elasto-viscous polymer melts). In the two limits of fast (elastic) deformation, or slow (viscous) deformation respectively, the deviatoric Cauchy stress may then be written

$$\hat{\boldsymbol{\sigma}} = \hat{\boldsymbol{\sigma}}(\hat{\boldsymbol{B}}, J), \text{ or } \hat{\boldsymbol{\sigma}} = \hat{\boldsymbol{\sigma}}(\hat{\boldsymbol{D}}, J) \tag{3}$$

respectively, where the two functions must be determined by experiment. In the general case of an intermediate rate (viscoelastic) deformation, we assume that "elastic" and

"viscous" deformation gradients exist, $\hat{\boldsymbol{F}}_{\mathrm{E}}$ and $\hat{\boldsymbol{F}}_{\mathrm{V}}$, such that the instantaneous Cauchy stress is given in terms of the left Cauchy-Green tensor and the rate of deformation derived from them respectively, thus

$$\hat{\boldsymbol{\sigma}} = \hat{\boldsymbol{\sigma}}(\hat{\boldsymbol{B}}_{\mathrm{E}}, J), \text{ and } \hat{\boldsymbol{\sigma}} = \hat{\boldsymbol{\sigma}}(\hat{\boldsymbol{D}}_{\mathrm{V}}, J). \tag{4}$$

Completion of a three-dimensional constitutive model requires knowledge of how $\hat{\boldsymbol{B}}_{\mathrm{E}}$ and $\hat{\boldsymbol{D}}_{\mathrm{V}}$ are related to $\hat{\boldsymbol{F}}$.

2.1 Approach based on additive decomposition of the velocity gradient (Approach I)

In this approach, additive decomposition of the isochoric velocity gradient $\hat{\boldsymbol{L}}$ into elastic $\hat{\boldsymbol{L}}_{\mathrm{E}}^{\mathrm{I}}$ and viscous $\hat{\boldsymbol{L}}_{\mathrm{V}}^{\mathrm{I}}$ parts is assumed *a priori*

$$\hat{\boldsymbol{L}} = \hat{\boldsymbol{L}}_{\mathrm{E}}^{\mathrm{I}} + \hat{\boldsymbol{L}}_{\mathrm{V}}^{\mathrm{I}}, \text{ hence } \hat{\boldsymbol{D}} = \hat{\boldsymbol{D}}_{\mathrm{E}}^{\mathrm{I}} + \hat{\boldsymbol{D}}_{\mathrm{V}}^{\mathrm{I}} \text{ and } \hat{\boldsymbol{W}} = \hat{\boldsymbol{W}}_{\mathrm{E}}^{\mathrm{I}} + \hat{\boldsymbol{W}}_{\mathrm{V}}^{\mathrm{I}}, \tag{5}$$

where superscript I is introduced to distinguish elastic and viscous quantities from their counterparts in approach II presented in the next section. The second of Eq. (5) expresses the additivity of rates of deformation proposed by Nemat-Nasser and others, where $\hat{\boldsymbol{D}}_{\mathrm{V}}^{\mathrm{I}}$ is defined by a flow rule (see Section 3).

There is no attempt to attribute precise physical meaning to $\hat{\boldsymbol{F}}_{\mathrm{E}}^{\mathrm{I}}$ and $\hat{\boldsymbol{F}}_{\mathrm{V}}^{\mathrm{I}}$ in terms of macroscopic response. In terms of polymer physics, $\hat{\boldsymbol{F}}_{\mathrm{E}}^{\mathrm{I}}$ relates to molecular chain configurations, whose perturbation from equilibrium at any instant gives rise to the entropic stress dependent on $\hat{\boldsymbol{B}}_{\mathrm{E}}^{\mathrm{I}}$. To exploit Eq.(5), we make use of the following kinematic identity for the time derivative of $\hat{\boldsymbol{B}}_{\mathrm{E}}^{\mathrm{I}}$ with respect to a fixed reference frame

$$\dot{\hat{\boldsymbol{B}}}_{\mathrm{E}}^{\mathrm{I}} = \left(\hat{\boldsymbol{F}}_{\mathrm{E}}^{\mathrm{I}}\left(\hat{\boldsymbol{F}}_{\mathrm{E}}^{\mathrm{I}}\right)^{\mathrm{T}}\right)^{\bullet} = \hat{\boldsymbol{L}}_{\mathrm{E}}^{\mathrm{I}}\hat{\boldsymbol{B}}_{\mathrm{E}}^{\mathrm{I}} + \hat{\boldsymbol{B}}_{\mathrm{E}}^{\mathrm{I}}\left(\hat{\boldsymbol{L}}_{\mathrm{E}}^{\mathrm{I}}\right)^{\mathrm{T}}, \tag{6}$$

where superscript T denotes the usual transpose, and the definition of the co-rotational (Jaumann) derivative of $\hat{\boldsymbol{B}}_{\mathrm{E}}^{\mathrm{I}}$

$$\overset{\circ}{\hat{\boldsymbol{B}}}_{\mathrm{E}}^{\mathrm{I}} \equiv \dot{\hat{\boldsymbol{B}}}_{\mathrm{E}}^{\mathrm{I}} - \hat{\boldsymbol{W}}\,\hat{\boldsymbol{B}}_{\mathrm{E}}^{\mathrm{I}} + \hat{\boldsymbol{B}}_{\mathrm{E}}^{\mathrm{I}}\,\hat{\boldsymbol{W}}\,. \tag{7}$$

There is no means of completing the model rigorously. An assumption must be made concerning apportionment of spin $\hat{\boldsymbol{W}}$ between elastic and viscous parts of the velocity gradient, in the third of Eq.(5). Here we consider two possible cases:

(i) Case 1: We follow Giesekus' plausible physical argument for polymers that $\hat{\boldsymbol{L}}_{\mathrm{V}}^{\mathrm{I}}$ must be an inner variable of the configurational state, as expressed by symmetric tensor $\hat{\boldsymbol{B}}_{\mathrm{E}}^{\mathrm{I}}$, and hence must itself be symmetric, giving $\hat{\boldsymbol{W}}_{\mathrm{V}}^{\mathrm{I}} = \boldsymbol{0}$ (Giesekus, 1982). Hence, it follows from Eq.(5) that $\hat{\boldsymbol{W}}_{\mathrm{E}}^{\mathrm{I}} = \hat{\boldsymbol{W}}$. Then, combining Eqs.(6)-(7) with the *a priori* assumption Eq.(5) gives

$$\left(\hat{\boldsymbol{B}}_{\mathrm{E}}^{\mathrm{I}}\right)^{\circ} = \hat{\boldsymbol{D}}_{\mathrm{E}}^{\mathrm{I}}\,\hat{\boldsymbol{B}}_{\mathrm{E}}^{\mathrm{I}} + \hat{\boldsymbol{B}}_{\mathrm{E}}^{\mathrm{I}}\,\hat{\boldsymbol{D}}_{\mathrm{E}}^{\mathrm{I}} = \left\{\hat{\boldsymbol{D}} - \hat{\boldsymbol{D}}_{\mathrm{V}}^{\mathrm{I}}\right\}\hat{\boldsymbol{B}}_{\mathrm{E}}^{\mathrm{I}} + \hat{\boldsymbol{B}}_{\mathrm{E}}^{\mathrm{I}}\left\{\hat{\boldsymbol{D}} - \hat{\boldsymbol{D}}_{\mathrm{V}}^{\mathrm{I}}\right\}. \tag{8}$$

We shall refer to Eq. (8) as the Leonov equation after its original proposer (Leonov, 1976). When constitutive representations are provided for $\hat{\boldsymbol{D}}_{\mathrm{V}}^{\mathrm{I}}$ and $\hat{\boldsymbol{B}}_{\mathrm{E}}^{\mathrm{I}}$ in terms of $\hat{\boldsymbol{\sigma}}$, Eq. (8) may be integrated to obtain the evolution of stress for a given deformation history. This approach has been used by Tervoort et al. (1998) in modelling elastic-viscoplastic deformation of glassy polymers.

(ii) Case 2: We assume that $\hat{\boldsymbol{W}}_{\mathrm{E}}^{\mathrm{I}} = \boldsymbol{0}$, hence $\hat{\boldsymbol{W}}_{\mathrm{V}}^{\mathrm{I}} = \hat{\boldsymbol{W}}$ and Eq.(8) is replaced by

$$\left(\hat{\boldsymbol{B}}_{\mathrm{E}}^{\mathrm{I}}\right)^{\bullet} = \hat{\boldsymbol{D}}_{\mathrm{E}}^{\mathrm{I}}\,\hat{\boldsymbol{B}}_{\mathrm{E}}^{\mathrm{I}} + \hat{\boldsymbol{B}}_{\mathrm{E}}^{\mathrm{I}}\,\hat{\boldsymbol{D}}_{\mathrm{E}}^{\mathrm{I}} = \left\{\hat{\boldsymbol{D}} - \hat{\boldsymbol{D}}_{\mathrm{V}}^{\mathrm{I}}\right\}\hat{\boldsymbol{B}}_{\mathrm{E}}^{\mathrm{I}} + \hat{\boldsymbol{B}}_{\mathrm{E}}^{\mathrm{I}}\left\{\hat{\boldsymbol{D}} - \hat{\boldsymbol{D}}_{\mathrm{V}}^{\mathrm{I}}\right\}. \tag{9}$$

2.2. Approach based on multiplicative decomposition of the deformation gradient (Approach II)

An alternative approach begins with the *a priori* presumption of multiplicative decomposition of the total isochoric deformation gradient. Thus, following Kröner (1960), Lee (1969) and many other authors

$$\hat{\boldsymbol{F}} = \hat{\boldsymbol{F}}_{\mathrm{E}}^{\mathrm{II}}\hat{\boldsymbol{F}}_{\mathrm{V}}^{\mathrm{II}}. \tag{10}$$

A physical interpretation of Eq.(10) is that, at any instant, $\hat{\boldsymbol{F}}_{\mathrm{V}}^{\mathrm{II}}$ is the permanent deformation that would remain on removal of the stress. In this case, kinematics gives the isochoric part of the velocity gradient as follows:

$$\hat{\boldsymbol{L}} = \dot{\hat{\boldsymbol{F}}} \left(\hat{\boldsymbol{F}}\right)^{-1} = \left(\hat{\boldsymbol{F}}_{\mathrm{E}}^{\mathrm{II}} \hat{\boldsymbol{F}}_{\mathrm{V}}^{\mathrm{II}}\right)^{\bullet} \left(\hat{\boldsymbol{F}}_{\mathrm{E}}^{\mathrm{II}} \hat{\boldsymbol{F}}_{\mathrm{V}}^{\mathrm{II}}\right)^{-1} = \tag{11}$$

$$= \dot{\hat{\boldsymbol{F}}}_{\mathrm{E}}^{\mathrm{II}} \left(\hat{\boldsymbol{F}}_{\mathrm{E}}^{\mathrm{II}}\right)^{-1} + \hat{\boldsymbol{F}}_{\mathrm{E}}^{\mathrm{II}} \dot{\hat{\boldsymbol{F}}}_{\mathrm{V}}^{\mathrm{II}} \left(\hat{\boldsymbol{F}}_{\mathrm{V}}^{\mathrm{II}}\right)^{-1} \left(\hat{\boldsymbol{F}}_{\mathrm{E}}^{\mathrm{II}}\right)^{-1} = \hat{\boldsymbol{L}}_{\mathrm{E}}^{\mathrm{II}} + \hat{\boldsymbol{F}}_{\mathrm{E}}^{\mathrm{II}} \hat{\boldsymbol{L}}_{\mathrm{V}}^{\mathrm{II}} \left(\hat{\boldsymbol{F}}_{\mathrm{E}}^{\mathrm{II}}\right)^{-1}$$

Then, we may extract the elastic part of the isochoric velocity gradient

$$\hat{\boldsymbol{L}}_{\mathrm{E}}^{\mathrm{II}} = \hat{\boldsymbol{L}} - \hat{\boldsymbol{F}}_{\mathrm{E}}^{\mathrm{II}} \hat{\boldsymbol{L}}_{\mathrm{V}}^{\mathrm{II}} \left(\hat{\boldsymbol{F}}_{\mathrm{E}}^{\mathrm{II}}\right)^{-1}, \tag{12}$$

and use it to determine the elastic part of the deformation gradient by solving the differential equation for $\hat{\boldsymbol{F}}_{\mathrm{E}}^{\mathrm{II}}$

$$\dot{\hat{\boldsymbol{F}}}_{\mathrm{E}}^{\mathrm{II}} = \hat{\boldsymbol{L}}\, \hat{\boldsymbol{F}}_{\mathrm{E}}^{\mathrm{II}} - \hat{\boldsymbol{F}}_{\mathrm{E}}^{\mathrm{II}} \hat{\boldsymbol{L}}_{\mathrm{V}}^{\mathrm{II}}, \tag{13}$$

to finally obtain the elastic part of the left Cauchy-Green tensor

$$\hat{\boldsymbol{B}}_{\mathrm{E}}^{\mathrm{II}} = \hat{\boldsymbol{F}}_{\mathrm{E}}^{\mathrm{II}} \left(\hat{\boldsymbol{F}}_{\mathrm{E}}^{\mathrm{II}}\right)^{\mathrm{T}}, \tag{14}$$

and hence the stress $\hat{\boldsymbol{\sigma}}$. Again, we find this cannot be completed rigorously, since $\hat{\boldsymbol{L}}_{\mathrm{V}}^{\mathrm{II}}$ appears in Eq.(13) but only its symmetric part $\hat{\boldsymbol{D}}_{\mathrm{V}}^{\mathrm{II}}$ is defined by the flow rule (see the next section). Once again, a decision is required on how to calculate the spin contribution to $\hat{\boldsymbol{L}}_{\mathrm{V}}^{\mathrm{II}}$. There exist some physically-based constitutive expressions for $\hat{\boldsymbol{W}}_{\mathrm{V}}^{\mathrm{II}}$ in the case of crystal-plasticity (see e.g. van der Giessen, 1991), but physics alone provides no similar expressions for amorphous polymers. Hence, an assumption must be made concerning $\hat{\boldsymbol{W}}_{\mathrm{V}}^{\mathrm{II}}$. Here we consider three cases, proposed by different authors for different situations.

(i) Case 1: We assume the viscous part $\hat{\boldsymbol{F}}_{\mathrm{V}}^{\mathrm{II}}$ of the deformation gradient is symmetric, hence it follows that $\hat{\boldsymbol{W}}_{\mathrm{V}}^{\mathrm{II}}$=0, and

$$\hat{\boldsymbol{L}}_{\mathrm{V}}^{\mathrm{II}} = \hat{\boldsymbol{D}}_{\mathrm{V}}^{\mathrm{II}}. \tag{15}$$

This is one of the cases considered by Boyce et al for describing elasto-plastic flow of glassy polymers (Boyce et al. 1989).

(ii) Case 2: We assume the elastic part $\hat{\boldsymbol{F}}_{\mathrm{E}}^{\mathrm{II}}$ of the deformation gradient is symmetric, $\hat{\boldsymbol{F}}_{\mathrm{E}}^{\mathrm{II}} = \left(\hat{\boldsymbol{F}}_{\mathrm{E}}^{\mathrm{II}}\right)^{\mathrm{T}}$ (Dafalias, 1987; Boyce et al., 1989; Reinhardt and Dubey, 1998). Then the

components of inelastic spin, expressed with respect to the principal axes of elastic stretch, can be shown to be

$$\hat{W}^{\mathrm{II}}_{(\mathrm{V})\,MN} = \hat{W}_{MN} - \frac{\hat{\lambda}^{\mathrm{II}}_{(\mathrm{E})M} - \hat{\lambda}^{\mathrm{II}}_{(\mathrm{E})N}}{\hat{\lambda}^{\mathrm{II}}_{(\mathrm{E})M} + \hat{\lambda}^{\mathrm{II}}_{(\mathrm{E})N}} \left\{ \hat{D}_{MN} + \hat{D}^{\mathrm{II}}_{(\mathrm{V})\,MN} \right\}, \tag{16}$$

where $\hat{\lambda}^{\mathrm{II}}_{(\mathrm{E})M,N}$ (M,N = 1..3) are the eigen values of the elastic left stretch tensor $\hat{\boldsymbol{V}}^{\mathrm{II}}_{\mathrm{E}} = \hat{\boldsymbol{F}}^{\mathrm{II}}_{\mathrm{E}}$ in this case.

(iii) Case 3: A convected viscous velocity gradient $\tilde{\hat{\boldsymbol{L}}}^{\mathrm{II}}_{\mathrm{V}}$ is defined, and assumed to be symmetric

$$\tilde{\hat{\boldsymbol{L}}}^{\mathrm{II}}_{\mathrm{V}} \equiv \hat{\boldsymbol{F}}^{\mathrm{II}}_{\mathrm{E}}\, \hat{\boldsymbol{L}}^{\mathrm{II}}_{\mathrm{V}} \left(\hat{\boldsymbol{F}}^{\mathrm{II}}_{\mathrm{E}} \right)^{-1} = \tilde{\hat{\boldsymbol{D}}}^{\mathrm{II}}_{\mathrm{V}}. \tag{17}$$

The corresponding rate of deformation tensor $\tilde{\hat{\boldsymbol{D}}}^{\mathrm{II}}_{\mathrm{V}}$ is chosen to be constitutively prescribed in terms of stress. Then, again, $\hat{\boldsymbol{F}}^{\mathrm{II}}_{\mathrm{E}}$ may be found by integration of its derivative via Eq.(12)

$$\dot{\hat{\boldsymbol{F}}}^{\mathrm{II}}_{\mathrm{E}} = \left(\hat{\boldsymbol{L}} - \tilde{\hat{\boldsymbol{D}}}^{\mathrm{II}}_{\mathrm{V}} \right) \hat{\boldsymbol{F}}^{\mathrm{II}}_{\mathrm{E}} \tag{18}$$

and from this $\hat{\boldsymbol{B}}^{\mathrm{II}}_{\mathrm{E}}$ and the stress $\hat{\boldsymbol{\sigma}}$ may be calculated. This approach was employed by Boyce et al. (2000), Dupaix and Boyce (2007) and Drozdov et al. (2008), when modelling highly elastic flows of polymer melts.

An interesting feature of Case 3 may be seen by using the transpose of Eq.(18) and Eq.(18) itself, to compute the time derivative of $\hat{\boldsymbol{B}}^{\mathrm{II}}_{\mathrm{E}}$ and hence

$$\mathring{\hat{\boldsymbol{B}}}^{\mathrm{II}}_{\mathrm{E}} = \hat{\boldsymbol{D}}^{\mathrm{II}}_{\mathrm{E}}\, \hat{\boldsymbol{B}}^{\mathrm{II}}_{\mathrm{E}} + \hat{\boldsymbol{B}}^{\mathrm{II}}_{\mathrm{E}}\, \hat{\boldsymbol{D}}^{\mathrm{II}}_{\mathrm{E}} = \left\{ \hat{\boldsymbol{D}} - \tilde{\hat{\boldsymbol{D}}}^{\mathrm{II}}_{\mathrm{V}} \right\} \hat{\boldsymbol{B}}^{\mathrm{II}}_{\mathrm{E}} + \hat{\boldsymbol{B}}^{\mathrm{II}}_{\mathrm{E}} \left\{ \hat{\boldsymbol{D}} - \tilde{\hat{\boldsymbol{D}}}^{\mathrm{II}}_{\mathrm{V}} \right\}. \tag{19}$$

Eq.(19) is close to Eq. (9) of approach I - case 1: the only difference is that $\tilde{\hat{\boldsymbol{D}}}^{\mathrm{II}}_{\mathrm{V}}$ replaces $\hat{\boldsymbol{D}}^{\mathrm{II}}_{\mathrm{V}}$.

3. Constitutive model

3.1. Linear viscoelastic model to study approaches 1 and 2

To expose the effects of different kinematic assumptions in the approaches outlined above, we consider the case of a hypothetical isotropic material that behaves physically as a compressible neo-Hookean solid in the elastic limit and a Newtonian fluid in the viscous limit. Then the Cauchy stress is related to J, $\hat{\boldsymbol{B}}_{\mathrm{E}}^{\mathrm{I}}$ (or $\hat{\boldsymbol{B}}_{\mathrm{E}}^{\mathrm{II}}$) and $\hat{\boldsymbol{D}}_{\mathrm{V}}^{\mathrm{I}}$ (or $\hat{\boldsymbol{D}}_{\mathrm{V}}^{\mathrm{II}}$, or $\tilde{\hat{\boldsymbol{D}}}_{\mathrm{V}}^{\mathrm{II}}$) as follows:

$$\boldsymbol{\sigma} = \sigma_{\mathrm{m}}\boldsymbol{1} + \hat{\boldsymbol{\sigma}} = K\log J\boldsymbol{1} + \frac{G}{J}\left\{\hat{\boldsymbol{B}}_{\mathrm{E}}^{\mathrm{I,II}} - \boldsymbol{1}\right\}, \tag{20}$$

$$\text{and } \hat{\boldsymbol{\sigma}} = 2\eta\hat{\boldsymbol{D}}_{\mathrm{V}}^{\mathrm{I,II}} \quad \text{or} \quad \hat{\boldsymbol{\sigma}} = 2\eta\tilde{\hat{\boldsymbol{D}}}_{\mathrm{V}}^{\mathrm{II}} \quad \text{(approach 2 - case 3 only)}, \tag{21}$$

where σ_{m}, K and G are the mean stress, bulk and shear modulus respectively; η is the Newtonian shear viscosity; $\boldsymbol{1}$ is the second-order identity tensor. Such a viscoelastic material has a characteristic time constant $\tau = \eta / G$.

3.2. Reference model – the Giesekus model

The particular constitutive model due to Giesekus (1982) provides a convenient benchmark for comparison of the approaches presented above. It is widely-used in describing polymer melt behaviour, where large elastic strains and rotations are present. In elastic and viscous limits it is neo-Hookean and Newtonian respectively, consistent with the material model described above. The Giesekus model is expressed in terms of the upper convected (Oldroyd) time derivative (Oldroyd, 1950; Giesekus, 1984) of the stress tensor, and in compressible form is

$$\tau J\overset{\triangledown}{\hat{\boldsymbol{\sigma}}} + \hat{\boldsymbol{\sigma}} + \frac{\alpha J\hat{\boldsymbol{\sigma}}\cdot\hat{\boldsymbol{\sigma}}}{\mathrm{G}} = 2\eta\hat{\boldsymbol{D}}\ \text{, where } \tau = \frac{\eta}{G} \tag{22}$$

$$\overset{\triangledown}{\hat{\boldsymbol{\sigma}}} = \dot{\hat{\boldsymbol{\sigma}}} - \hat{\boldsymbol{L}}\hat{\boldsymbol{\sigma}} - \hat{\boldsymbol{\sigma}}\hat{\boldsymbol{L}}^{\mathrm{T}} \tag{23}$$

$$\boldsymbol{\sigma} = K\log J\boldsymbol{1} + \hat{\boldsymbol{\sigma}}, \tag{24}$$

The adjustable parameter α is helpful in fitting experimental data in the viscoelastic regime. The limit $\alpha = 0$ corresponds to the upper convected Maxwell model (UCM). But

the UCM is well-known to have several weaknesses when compared to experimental data for polymer melts (Larson, 1988). Several of these are side-stepped by taking $\alpha > 0$. For example, unphysical stress growth at high rates of extensional flow is avoided*, and the observed stress overshoot in start-up shear flows is predicted naturally. Interestingly, the case $\alpha = 1$ can be shown to be identical to the Leonov equation combined with the model in Section 3.1 – see Appendix A.

4. Case studies and discussion

The behaviours of the various models were compared by means of a number of case study simulations. For that purpose a series of constitutive models based on each of the approaches I and II outlined above, together with Eqs. (20) and (21), were implemented as user-defined material subroutines, and solved numerically using the FEM-based package (ABAQUS/Standard) for a single element, as a convenient solver. The simple Euler method was used to calculate the elastic part of the deformation gradient from the rate equation provided by each kinematic approach. The Giesekus model (Eqs (22) – (24)) was implemented similarly. Table 1 contains the numerical values of model parameters employed throughout. The specific values were measured in a recent study of poly(ethylene terephthalate) in the authors' laboratory, in the temperature region characteristic of industrial processes such as thermoforming of sheets and injection stretch-blow moulding of bottles. They are typical of amorphous thermoplastic polymers in highly elastic flows at temperatures above the glass transition.

Table 1. Model parameters

Property	Value
Bulk modulus K	1.8 GPa
Shear modulus G	3.29MPa
Viscosity η	16.5 MPa s

* The UCM predicts that no steady state flow can be achieved in uniaxial extension, for true strain-rates greater than $1/2\tau$.

From Table 1, the time constant in all cases was $\tau = 5.0$ s. Two loading conditions were considered: (1) uniaxial elongation at constant extension rate, and (2) simple shear at constant shear rate.

Figure 1 shows the example of uniaxial extension in the 1-direction (horizontal), at an extension rate of 0.4 s^{-1}. In this case no rotations are expected. Hence, approaches I and II (cases 1 and 2) gave identical predictions. As expected from Eq.(19) and Appendix A, approach II – case 3 and the Giesekus model for α=1.0 coincide with predictions of approach I – case 1, and hence they are not shown in Figure 1 and subsequent figures. Predictions made with the Giesekus model and lower values of α agree only up to applied extensions ~ 1. The exaggerated prediction of stress for the UCM case ($\alpha = 0$) is clearly in evidence. Figure 2 shows the predicted stress plotted as extensional viscosity $\sigma_{11} / \dot{\varepsilon}$ versus time (with logarithmic scales) for three extension-rates 0.04, 0.4 and 4 s^{-1}. At the highest rate the UCM case reveals unphysical growth of stress, for which it is well-known (Larson, 1988). An obvious conclusion is that approaches I (all 2 cases) and II (all 3 cases), and the Giesekus model with $\alpha = 1$ can be used interchangeably when no rigid body rotation is involved.

To discriminate between the approaches, simple shear tests in the 1-2 plane were simulated, with displacement in the 1-direction. Predictions of shear stress for a shear rate of 0.4 s^{-1} are shown in Figure 3. Interestingly, discrepancies (similarities) between some cases of approach I and II now appear, depending on the definition of the inelastic spin. All approaches and models agree up to applied shear $\gamma \sim 1$. Then, approach I – case 2 does not predict the stress overshoot, observed experimentally (Larson, 1988), and follows to some extent the Giesekus model with $\alpha = 0.0$. Further, approach II - case 1 predicts a rapid increase of shear stress, failing to converge on a steady state, and hence at variance with experimental observations. Interestingly, approach II - case 2 recovers the results of approach I. In fact, it can be shown analytically (see Appendix B), that approach II - case 2 is equivalent to approach II - case 3 (identical to approach I – case 1) in the case of simple shear. However, this situation might not hold in general, e.g. if the uniaxial tension and shear are superimposed.

Another comment might be made in relation to approach II – case 2 . The off-diagonal components of $\hat{D}^{\mathrm{II}}_{(\mathrm{V})\,MN}$ (Eq.(16)) are zero since $\hat{\boldsymbol{D}}^{\mathrm{II}}_{(\mathrm{V})}$ is determined from a flow rule using a stress tensor (see Eq.(21)), which becomes diagonal when transformed to the axes of $\hat{\lambda}^{\mathrm{II}}_{(\mathrm{E})M,N}$. Hence, $\hat{W}^{\mathrm{II}}_{(\mathrm{V})\,MN}$ is unaffected by $\hat{D}^{\mathrm{II}}_{(\mathrm{V})\,MN}$ and Eq.(16) provides the same results as the approach proposed for elastic-plastic deformation of metals by Reinhardt and Dubey (1998), provided that their modified spin $\hat{\boldsymbol{W}}^{*}_{\mathrm{V}}$ satisfies $\hat{\boldsymbol{W}}^{*}_{\mathrm{V}} = \hat{\boldsymbol{W}}^{\mathrm{II}}_{\mathrm{V}}$.

Hence, approach I – case 1 (and the identical approach II – case 3, and Giesekus model with α = 1), along with approach II - case 2, all show a stress overshoot before arriving at the steady state, as observed experimentally (Larson, 1988).

Also of interest in relation to simple shear deformation are the normal stresses that accompany it. The first normal stress difference is defined $N_1 = \sigma_{11} - \sigma_{22}$. This difference is frequently measured for polymer melts and gives rise to a force that tends to separate (or pull together) the shearing plates in a simple shear experiment. Here N_1 is predicted to be positive, in agreement with experiment, and hence it tends to push apart the shearing plates. Typical experimental data show a steady-state being reached, preceded by an overshoot at highest strain rates (Larson, 1988). As shown in Figure 4, approach I – case 1 (and the identical approach II - case 3 and the Giesekus model with α = 1) and also case 2 of approach II agree qualitatively with experiment. However, it may be seen that a zero value of N_1 is obtained (i.e. $\sigma_{11} = \sigma_{22}$) with approach I – case 2 (i.e. $\hat{\boldsymbol{W}}^{\mathrm{I}}_{\mathrm{E}} = \boldsymbol{0}$), and also no steady-state is reached using approach II - case 1 (i.e. $\hat{\boldsymbol{W}}^{\mathrm{II}}_{\mathrm{V}} = \boldsymbol{0}$). Hence, again we see the critical importance of the assignment of viscous spin if approach I and approach II are to be employed. Predictions of the Giesekus model with α = 0 and 0.5 are shown in Figure 4 for completeness. They show the correct qualitative trend, differing in the magnitude of N_1 predicted.

The predicted second normal stress difference $N_2 = \sigma_{22} - \sigma_{33}$ is shown in Figure 5. Again approach I – case 1 (identical approach II – case 3 and the Giesekus model with α = 1) and approach II – case 2 predict correctly the observed trend of tending towards a steady (in this case, negative) value. And again approach I – case 2 and approach II - case 1 shows an unphysical divergence of stress, and moreover its sign is predicted to be

positive, at variance with experiment. The Giesekus model again gives the correct trend, and shows a steady state value of N_2 that is highly sensitive to α. The Giesekus model (α = 0) predicts N_2 = 0, while α = 0.5 gives a steady state value $N_2 \sim -N_1/4$ typical of experimental data (Dealy and Larson, 2006).

The variation of shear response with shear rate is shown in Figure 6 for three shear rates. approach I – case 1 (identical approach II – cases 2 and 3 and the Giesekus model (α > 0)) reproduce correctly the trends seen in experimental data: a stress overshoot that increases with strain-rate, and a steady-state viscosity that decreases with increasing strain-rate (i.e. shear-thinning) (Larson, 1988). It is worth emphasising the difference between the responses in shear and extension. Approach I – case 1, combined with the model of Section 3.1, is intrinsically Newtonian in steady-state uniaxial extension: the steady-state elongational viscosity is independent of extension-rate. But the same model shows a shear viscosity that decreases with increasing shear-rate. The difference is clearly a consequence of the finite rotations occurring during shear deformation and their absence during extension, and hence arises directly from the kinematic structure of the model. However, approach I – case 2 shows that in the presence of viscous spin, the shear viscosity will be over-predicted with increasing strain rate, as shown for $\dot{\gamma} = 4\text{s}^{-1}$ Figure 6 also includes the prediction for approach II case 1, but this can be seen to depart dramatically from the pattern observed experimentally, at all shear-rates. As may be seen, at the lowest rate, grossly unphysical behaviour is observed. Multiple simulations with varying time-step size confirmed that the wild divergence of predicted viscosity is a genuine feature of the model and not an artefact of the numerical integration of it.

5. Conclusions

Two approaches to the kinematic structuring of constitutive models for highly elastic flows of polymer melts have been examined systematically: assuming additivity of elastic and viscous velocity gradients, or assuming multiplicability of their deformation gradients. A series of constitutive models was compared, with differing kinematic structure but the same linear responses in elastic and viscous limits. They were solved numerically and their predictions compared, and they were also compared to those of the

Giesekus model. Differences between the approaches appear only in the presence of finite rotations. Three clear results emerge.

First, the approach of assuming additivity of elastic and viscous velocity gradients, and symmetry of the latter (i.e. approach I – case 1), produces viscoelastic response qualitatively in agreement with experiment. However, the same additivity assumption, but with a symmetric elastic velocity gradient (i.e. approach I – case 2) leads to unphysical predictions of the normal stress differences and sometimes shear flow thickening.

Second, the approach of assuming multiplicability of elastic and viscous deformation gradients, and symmetry of the viscous deformation gradient, (approach II - case 1) is not satisfactory: it predicts behaviour grossly at variance with experimental observations on polymer melts in shear flows, when the shear exceeds approximately unity. The predictions of shear stress and the first and second normal stress differences all show major errors.

Third, however, alternatives to approach II – case 1 assume: (1) symmetry of the elastic deformation gradient, which leads to a closed-form expression for the inelastic spin in principal axes of the elastic stretch (approach II - case 2), or (2) the viscous velocity gradient, when convected to the current configuration, is symmetric and constitutively defined by the viscous-limit flow rule (approach II - case 3). In both cases, the model is then indistinguishable from approach I – case 1 in uniaxial extension and simple shear. However, approach II – case 2 may not agree with approach I – case 1 in a general case, if e.g. extension and shear are superimposed. Furthermore, approach I – case 1 and approach II – case 3, when the elastic and viscous limits are neo-Hookean and Newtonian respectively, are indistinguishable from the Giesekus model with $\alpha = 1$.

The major conclusion of this work is that, for consistency with experimental data, empirical constitutive models for highly elastic flows of polymer melts should be based on the kinematic structures of approach I – case 1, or its equivalent approach II - case 3.

Acknowledgements

The authors thank Professor F.P.E. Dunne (University of Oxford) for helpful discussions. The work was supported by Research Grant EP/C006984/1 from the Engineering and Physical Sciences Research Council.

References

A.M. Adams, C.P. Buckley, D.P. Jones, Biaxial hot drawing of poly(ethylene terephthalate): measurements and modelling of strain-stiffening. Polymer 41 (2000), 771-786.

G. Astarita, G. Marrucci, Principles of Non-newtonian fluid mechanics, McGraw-Hill, 1974.

M.C. Boyce, G.G. Weber, D.M. Parks, On the kinematics of finite strain plasticity. Journal of the Mechanics and Physics of Solids 37(5), 647-665, 1989.

M.C. Boyce, S. Socrate, P.G. Llana, Constitutive behaviour for the finite deformation stress-strain behaviour poly(ethylene terephthalate) above the glass transition, Polymer, 41 (2000), 2183-2201.

R.B. Dupaix, M.C. Boyce, Constitutive modelling of the finite strain behaviour of amorphous polymers in and above glass transition. Mechanics of Materials 39(2007), 39-52.

L. Chevalier, Y. Marco, Identification of a strain induced crystallisation model for PET under uni- and bi-axial loading: Influence of temperature dispersion. Mechanics of Materials 39 (2007), 596-609.

Y.F. Dafalias, Issues on the Constitutive Formulation at Large Elastoplastic Deformations, Part 1: Kinematics. Acta Mechanica, 69 (1997), 119-138.

J.M. Deally, R.G. Larson, Structure and rheology of molten polymers. Hanser Gardner Publications, 2006.

P.J. Dooling, C.P. Buckley, S. Rostami, N. Zahlan, Hot-drawing of poly(methyl methacrylate) and simulation using a glass-rubber constitutive model. Polymer 43 (2002), 2451-2465.

A. Doufas, A.J. McHugh, C. Miller, Simulation of melt-spinning including flow-induced crystallization. Part 1. Model development and predictions. 92(2000), 27-66.

A.D. Drozdov, E.A. Jensen, J. de C. Christiansen, Thermo-viscoelasticity of polymer melts: experiments and modeling. Acta Mechanica 197, 211-245, 2008.

R.B. Dupaix, M.C. Boyce, Constitutive modelling of the finite strain behaviour of amorphous polymers in and above the glass transition. Mechanics of Materials, 39 (2007), 39-52.

P.J. Flory, Thermodynamic relations for high elastic materials, Transactions of the Faraday Society, 57 (1961) 829-838.

H. Giesekus, A simple constitutive equation for polymer fluids based on the concept of deformation-dependent tensorial mobility. Journal of Non-Newtonian Fluid Mechanics, 11 (1982), 69-109.

H. Giesekus, On configuration-dependent generalized Oldroyd derivatives, Journal of Non-Newtonian Fluid Mechanics, 14 (1984), 47-65.

C. G'Sell, J.J. Jonas, Determination of the plastic behaviour of solid polymers at constant true strain rate. Journal of Materials Science 14(1979), 583-591.

E. Kröner, Allgemeine Kontinuumstheorie der Versetzungen und Eigenspannungen. Archive for Rational Mechanics and Analysis, 4 (1960), 273-334.

A.E. Likhtman, R.S. Graham, Simple constitutive equation for linear polymer melts derived from molecular theory: Rolie-Poly equation. Journal of Non-Newtonian Fluid Mechanics 114(2003), 1-12.

R.G. Larson, Elongational-flow predictions of the Leonov constitutive equation. Rheologica Acta 22 (1983), 435-448.

R.G. Larson, Constitutive equations for polymer melts and solutions. Butterworths, 1988.

E.H. Lee, Elastic-plastic deformation at finite strains. Journal of Applied Mechanics, 36 (1969), 1-6.

A.I. Leonov, Nonequilibrium thermodynamics and rheology of viscoelastic polymer media, Rheologica Acta, 15(2) (1976), 85-98.

A. Makradi, S. Ahzi, R.V. Gregory, D.D. Edie, A two-phase self-consistent model for the deformation and phase transformation behaviour of polymers above the glass transition temperature: application to PET. International Journal of Plasticity 21 (2005), 741-758.

R.G. Matthews, R.A. Duckett, I.M. Ward, D.P. Jones, The biaxial drawing behaviour of poly(ethylene terephthalate). Polymer 38(9) (1997), 4795-4802.

T.C.B. McLeish, R.G. Larson, Molecular constitutive equations for a class of branched polymers: The pom-pom polymer. Journal of Rheology, 42(1998), 81-110.

S. Nemat-Nasser, Decomposition of strain measures and their rates in finite deformation elastoplasticity, International Journal of Solids and Structures, 15 (1979), 155-166.

S. Nemat-Nasser, On finite deformation elasto-plasticity, International Journal of Solids and Structures, 18(10) (1982), 857-872.

J.G. Oldroyd, On the formulation of the rheological equations of state. Proceedings of the Royal Society of London A. 200(1063) (1950), 523-541.

A. Poitou, A. Ammar, Y. Marco, L. Chevalier, M. Chaouche, Crystallization of polymers under strain: from molecular properties to macroscopic models. Computer Methods in Applied Mechanics and Engineering, 192 (2003), 3245-3264.

W.D. Reinhardt, R.N. Dubey, An Eulerian-based approach to elastic-plastic decomposition, Acta Mechanica, 131 (1998), 111-119.

J.D. Ferry, Viscoelastic properties of polymers of polymers, 3rd edition, Wiley, 1980.

J. Sweeney, I.M. Ward, Rate-dependent and network phenomena in the multiaxial drawing of poly(vinyl chloride). Polymer 36(2) 1995, 299-308.

T.A. Tervoort, R.J.M. Smit, W.A.M. Brekelmans, L.E. Govaert, A constitutive equation for the elasto-viscoplastic deformation of glassy polymers, Mechanics of Time-Dependent Materials, 1 (1998), 269-291.

E. Van der Giessen, Micromechanical and thermodynamic aspects of the plastic spin. International Journal of Plasticity, 7 (1991), 365-386.

M. Vigny, A. Aubert, J.M. Hiver, M. Aboulfaraj, C. G'Sell, Constitutive viscoplastic behavior of amorphous PET during plane-strain tensile stretching. Polymer Engineering and Science, 39(12) (1999), 2366-2376.

Appendix A: *Proof of the equivalence between approach I – case 1, and the Giesekus model with $\alpha = 1$.*

Combining the upper convected derivative of the elastic part of the left Cauchy-Green tensor is (Larson, 1983)

$$\overset{\nabla}{\hat{\boldsymbol{B}}}_{\mathrm{E}}^{\mathrm{I}} \equiv \overset{\circ}{\hat{\boldsymbol{B}}}_{\mathrm{E}}^{\mathrm{I}} - \hat{\boldsymbol{B}}_{\mathrm{E}}^{\mathrm{I}}\hat{\boldsymbol{D}} - \hat{\boldsymbol{B}}_{\mathrm{E}}^{\mathrm{I}}\hat{\boldsymbol{D}} \text{ , where } \hat{\boldsymbol{D}} = \hat{\boldsymbol{D}}_{\mathrm{E}}^{\mathrm{I}} + \hat{\boldsymbol{D}}_{\mathrm{V}}^{\mathrm{I}} \tag{A1}$$

with the kinematic identity of Leonov (Larson, 1983)

$$\overset{\circ}{\hat{\boldsymbol{B}}}_{\mathrm{E}}^{\mathrm{I}} - \hat{\boldsymbol{B}}_{\mathrm{E}}^{\mathrm{I}}\hat{\boldsymbol{D}}_{\mathrm{E}}^{\mathrm{I}} - \hat{\boldsymbol{D}}_{\mathrm{E}}^{\mathrm{I}}\hat{\boldsymbol{B}}_{\mathrm{E}}^{\mathrm{I}} = \boldsymbol{0}, \tag{A2}$$

one arrives at

$$\overset{\nabla}{\hat{\boldsymbol{B}}}_{\mathrm{E}}^{\mathrm{I}} + \hat{\boldsymbol{B}}_{\mathrm{E}}^{\mathrm{I}}\hat{\boldsymbol{D}}_{\mathrm{V}}^{\mathrm{I}} + \hat{\boldsymbol{D}}_{\mathrm{V}}^{\mathrm{I}}\hat{\boldsymbol{B}}_{\mathrm{E}}^{\mathrm{I}} = \boldsymbol{0}. \tag{A3}$$

Substitution of the isochoric part of the stress tensor from Eqs (20) and (21) into equation A3 gives

$$\frac{\tau}{\eta} J \overset{\nabla}{\hat{\boldsymbol{\sigma}}} + \overset{\nabla}{\boldsymbol{1}} + \frac{1}{\eta}\left\{\frac{\tau}{\eta} J\hat{\boldsymbol{\sigma}}\cdot\hat{\boldsymbol{\sigma}} + \hat{\boldsymbol{\sigma}}\right\} = \boldsymbol{0}, \text{ and } \frac{\tau}{\eta} = \frac{1}{\mathrm{G}} \tag{A4}$$

where $\overset{\nabla}{\boldsymbol{1}} = -2\hat{\boldsymbol{D}}$ (and $\boldsymbol{1}$ denotes a second-order identity tensor), hence finally Eq. (A4) becomes

$$\tau J \overset{\nabla}{\hat{\boldsymbol{\sigma}}} + \frac{1}{\mathrm{G}} J\hat{\boldsymbol{\sigma}}\cdot\hat{\boldsymbol{\sigma}} + \hat{\boldsymbol{\sigma}} = 2\eta\hat{\boldsymbol{D}}, \tag{A5}$$

which is equivalent to Eq. (22) for $\alpha = 1$.

Appendix B: *On the connection between cases 2 and 3 of the approach II.*

Firstly, let us consider approach II-case 2, hence assume $\left(\hat{\boldsymbol{F}}_{\mathrm{E}}^{\mathrm{II}}\right)^{\mathrm{T}} = \hat{\boldsymbol{F}}_{\mathrm{E}}^{\mathrm{II}}$ and $\hat{\boldsymbol{F}}_{\mathrm{E}}^{\mathrm{II}} = \hat{\boldsymbol{V}}_{\mathrm{E}}^{\mathrm{II}}$.

The time derivative of the elastic deformation gradient and its transpose can be expressed as

$$\dot{\hat{\boldsymbol{F}}}_{\mathrm{E}}^{\mathrm{II}} = \hat{\boldsymbol{L}}\,\hat{\boldsymbol{F}}_{\mathrm{E}}^{\mathrm{II}} - \hat{\boldsymbol{F}}_{\mathrm{E}}^{\mathrm{II}}\hat{\boldsymbol{L}}_{\mathrm{V}}^{\mathrm{II}} \text{ and } \left(\dot{\hat{\boldsymbol{F}}}_{\mathrm{E}}^{\mathrm{II}}\right)^{\mathrm{T}} = \hat{\boldsymbol{F}}_{\mathrm{E}}^{\mathrm{II}}\left(\hat{\boldsymbol{L}}\right)^{\mathrm{T}} - \left(\hat{\boldsymbol{L}}_{\mathrm{V}}^{\mathrm{II}}\right)^{\mathrm{T}}\hat{\boldsymbol{F}}_{\mathrm{E}}^{\mathrm{II}} \tag{B1}$$

Now let us consider the material time derivative of the elastic left Cauchy-Green tensor – hence using Eq.(B1)

$$\dot{\hat{\boldsymbol{B}}}_{\mathrm{E}}^{\mathrm{II}} = \dot{\hat{\boldsymbol{F}}}_{\mathrm{E}}^{\mathrm{II}}\left(\hat{\boldsymbol{F}}_{\mathrm{E}}^{\mathrm{II}}\right)^{\mathrm{T}} + \hat{\boldsymbol{F}}_{\mathrm{E}}^{\mathrm{II}}\left(\dot{\hat{\boldsymbol{F}}}_{\mathrm{E}}^{\mathrm{II}}\right)^{\mathrm{T}} = \hat{\boldsymbol{L}}\hat{\boldsymbol{F}}_{\mathrm{E}}^{\mathrm{II}}\hat{\boldsymbol{F}}_{\mathrm{E}}^{\mathrm{II}} + \hat{\boldsymbol{F}}_{\mathrm{E}}^{\mathrm{II}}\hat{\boldsymbol{F}}_{\mathrm{E}}^{\mathrm{II}}\hat{\boldsymbol{L}}^{\mathrm{T}} - \hat{\boldsymbol{F}}_{\mathrm{E}}^{\mathrm{II}}\left(\hat{\boldsymbol{L}}_{\mathrm{V}}^{\mathrm{II}} + \left(\hat{\boldsymbol{L}}_{\mathrm{V}}^{\mathrm{II}}\right)^{\mathrm{T}}\right)\hat{\boldsymbol{F}}_{\mathrm{E}}^{\mathrm{II}} = \tag{B2}$$

$$= \hat{\boldsymbol{L}}\hat{\boldsymbol{V}}_{\mathrm{E}}^{\mathrm{II}}\hat{\boldsymbol{V}}_{\mathrm{E}}^{\mathrm{II}} + \hat{\boldsymbol{V}}_{\mathrm{E}}^{\mathrm{II}}\hat{\boldsymbol{V}}_{\mathrm{E}}^{\mathrm{II}}\hat{\boldsymbol{L}}^{\mathrm{T}} - 2\hat{\boldsymbol{V}}_{\mathrm{E}}^{\mathrm{II}}\hat{\boldsymbol{D}}_{\mathrm{V}}^{\mathrm{II}}\hat{\boldsymbol{V}}_{\mathrm{E}}^{\mathrm{II}} = \hat{\boldsymbol{L}}\hat{\boldsymbol{B}}_{\mathrm{E}}^{\mathrm{II}} + \hat{\boldsymbol{B}}_{\mathrm{E}}^{\mathrm{II}}\hat{\boldsymbol{L}}^{\mathrm{T}} - 2\hat{\boldsymbol{V}}_{\mathrm{E}}^{\mathrm{II}}\hat{\boldsymbol{D}}_{\mathrm{V}}^{\mathrm{II}}\hat{\boldsymbol{V}}_{\mathrm{E}}^{\mathrm{II}} =$$

$$= \left(\hat{\boldsymbol{D}} + \hat{\boldsymbol{W}}\right)\hat{\boldsymbol{B}}_{\mathrm{E}}^{\mathrm{II}} + \hat{\boldsymbol{B}}_{\mathrm{E}}^{\mathrm{II}}\left(\hat{\boldsymbol{D}} - \hat{\boldsymbol{W}}\right) - 2\hat{\boldsymbol{V}}_{\mathrm{E}}^{\mathrm{II}}\hat{\boldsymbol{D}}_{\mathrm{V}}^{\mathrm{II}}\hat{\boldsymbol{V}}_{\mathrm{E}}^{\mathrm{II}} =$$

$$= \hat{\boldsymbol{D}}\hat{\boldsymbol{B}}_{\mathrm{E}}^{\mathrm{II}} + \hat{\boldsymbol{B}}_{\mathrm{E}}^{\mathrm{II}}\hat{\boldsymbol{D}} + \hat{\boldsymbol{W}}\hat{\boldsymbol{B}}_{\mathrm{E}}^{\mathrm{II}} - \hat{\boldsymbol{B}}_{\mathrm{E}}^{\mathrm{II}}\hat{\boldsymbol{W}} - 2\hat{\boldsymbol{V}}_{\mathrm{E}}^{\mathrm{II}}\hat{\boldsymbol{D}}_{\mathrm{V}}^{\mathrm{II}}\hat{\boldsymbol{V}}_{\mathrm{E}}^{\mathrm{II}}.$$

Secondly, let us consider approach II - case 3, where the material time derivative of elastic deformation gradient is

$$\dot{\hat{\boldsymbol{F}}}_{\mathrm{E}}^{\mathrm{II}} = \hat{\boldsymbol{L}}\hat{\boldsymbol{F}}_{\mathrm{E}}^{\mathrm{II}} - \tilde{\hat{\boldsymbol{L}}}_{\mathrm{V}}\hat{\boldsymbol{F}}_{\mathrm{E}}^{\mathrm{II}} \text{ and } \left(\dot{\hat{\boldsymbol{F}}}_{\mathrm{E}}^{\mathrm{II}}\right)^{\mathrm{T}} = \left(\hat{\boldsymbol{F}}_{\mathrm{E}}^{\mathrm{II}}\right)^{\mathrm{T}}\hat{\boldsymbol{L}}^{\mathrm{T}} - \left(\hat{\boldsymbol{F}}_{\mathrm{E}}^{\mathrm{II}}\right)^{\mathrm{T}}\left(\tilde{\hat{\boldsymbol{L}}}_{\mathrm{V}}^{\mathrm{II}}\right)^{\mathrm{T}}, \text{ where } \tilde{\hat{\boldsymbol{L}}}_{\mathrm{V}}^{\mathrm{II}} = \tilde{\hat{\boldsymbol{D}}}_{\mathrm{V}}^{\mathrm{II}} \tag{B3}$$

Then, consider the time derivative of $\hat{\boldsymbol{B}}_{\mathrm{E}}^{\mathrm{II}}$

$$\dot{\hat{\boldsymbol{B}}}_{\mathrm{E}}^{\mathrm{II}} = \dot{\hat{\boldsymbol{F}}}_{\mathrm{E}}^{\mathrm{II}}\left(\hat{\boldsymbol{F}}_{\mathrm{E}}^{\mathrm{II}}\right)^{\mathrm{T}} + \hat{\boldsymbol{F}}_{\mathrm{E}}^{\mathrm{II}}\left(\dot{\hat{\boldsymbol{F}}}_{\mathrm{E}}^{\mathrm{II}}\right)^{\mathrm{T}} = \tag{B4}$$

$$= \hat{\boldsymbol{L}}\hat{\boldsymbol{F}}_{\mathrm{E}}^{\mathrm{II}}\left(\hat{\boldsymbol{F}}_{\mathrm{E}}^{\mathrm{II}}\right)^{\mathrm{T}} - \tilde{\hat{\boldsymbol{L}}}_{\mathrm{V}}^{\mathrm{II}}\hat{\boldsymbol{F}}_{\mathrm{E}}^{\mathrm{II}}\left(\hat{\boldsymbol{F}}_{\mathrm{E}}^{\mathrm{II}}\right)^{\mathrm{T}} + \hat{\boldsymbol{F}}_{\mathrm{E}}^{\mathrm{II}}\left(\hat{\boldsymbol{F}}_{\mathrm{E}}^{\mathrm{II}}\right)^{\mathrm{T}}\hat{\boldsymbol{L}}^{\mathrm{T}} - \hat{\boldsymbol{F}}_{\mathrm{E}}^{\mathrm{II}}\left(\hat{\boldsymbol{F}}_{\mathrm{E}}^{\mathrm{II}}\right)^{\mathrm{T}}\left(\tilde{\hat{\boldsymbol{L}}}_{\mathrm{V}}^{\mathrm{II}}\right)^{\mathrm{T}} =$$

$$= \left(\hat{\boldsymbol{D}} + \hat{\boldsymbol{W}}\right)\hat{\boldsymbol{B}}_{\mathrm{E}}^{\mathrm{II}} - \tilde{\hat{\boldsymbol{D}}}_{\mathrm{V}}^{\mathrm{II}}\hat{\boldsymbol{B}}_{\mathrm{E}}^{\mathrm{II}} + \hat{\boldsymbol{B}}_{\mathrm{E}}^{\mathrm{II}}\left(\hat{\boldsymbol{D}} - \hat{\boldsymbol{W}}\right) - \hat{\boldsymbol{B}}_{\mathrm{E}}^{\mathrm{II}}\tilde{\hat{\boldsymbol{D}}}_{\mathrm{V}}^{\mathrm{II}} =$$

$$= \hat{\boldsymbol{D}}\hat{\boldsymbol{B}}_{\mathrm{E}}^{\mathrm{II}} + \hat{\boldsymbol{B}}_{\mathrm{E}}^{\mathrm{II}}\hat{\boldsymbol{D}} + \hat{\boldsymbol{W}}\hat{\boldsymbol{B}}_{\mathrm{E}}^{\mathrm{II}} - \hat{\boldsymbol{B}}_{\mathrm{E}}^{\mathrm{II}}\hat{\boldsymbol{W}} - \tilde{\hat{\boldsymbol{D}}}_{\mathrm{V}}^{\mathrm{II}}\hat{\boldsymbol{V}}_{\mathrm{E}}^{\mathrm{II}}\hat{\boldsymbol{V}}_{\mathrm{E}}^{\mathrm{II}} - \hat{\boldsymbol{V}}_{\mathrm{E}}^{\mathrm{II}}\hat{\boldsymbol{V}}_{\mathrm{E}}^{\mathrm{II}}\tilde{\hat{\boldsymbol{D}}}_{\mathrm{V}}^{\mathrm{II}}$$

Since

$$\left(\tilde{\hat{\boldsymbol{D}}}_{\mathrm{V}}^{\mathrm{II}}\hat{\boldsymbol{V}}_{\mathrm{E}}^{\mathrm{II}}\hat{\boldsymbol{V}}_{\mathrm{E}}^{\mathrm{II}}\right)^{\mathrm{T}} = \hat{\boldsymbol{V}}_{\mathrm{E}}^{\mathrm{II}}\hat{\boldsymbol{V}}_{\mathrm{E}}^{\mathrm{II}}\tilde{\hat{\boldsymbol{D}}}_{\mathrm{V}}^{\mathrm{II}} \tag{B5}$$

then, Eq.(B4) can be given by

$$\dot{\hat{\boldsymbol{B}}}_{\mathrm{E}}^{\mathrm{II}} = \hat{\boldsymbol{D}}\hat{\boldsymbol{B}}_{\mathrm{E}}^{\mathrm{II}} + \hat{\boldsymbol{B}}_{\mathrm{E}}^{\mathrm{II}}\hat{\boldsymbol{D}} + \hat{\boldsymbol{W}}\hat{\boldsymbol{B}}_{\mathrm{E}}^{\mathrm{II}} - \hat{\boldsymbol{B}}_{\mathrm{E}}^{\mathrm{II}}\hat{\boldsymbol{W}} - 2\tilde{\hat{\boldsymbol{D}}}_{\mathrm{V}}^{\mathrm{II}}\hat{\boldsymbol{V}}_{\mathrm{E}}^{\mathrm{II}}\hat{\boldsymbol{V}}_{\mathrm{E}}^{\mathrm{II}} \tag{B6}$$

Hence, by comparing Eq.(B2) of case 2 with Eq.(B6) of case 3, it is clear that both approaches are identical if

$$\hat{\boldsymbol{V}}_{\mathrm{E}}^{\mathrm{II}}\hat{\boldsymbol{D}}_{\mathrm{V}}^{\mathrm{II}}\hat{\boldsymbol{V}}_{\mathrm{E}}^{\mathrm{II}} = \tilde{\hat{\boldsymbol{D}}}_{\mathrm{V}}^{\mathrm{II}}\hat{\boldsymbol{V}}_{\mathrm{E}}^{\mathrm{II}}\hat{\boldsymbol{V}}_{\mathrm{E}}^{\mathrm{II}}. \tag{B7}$$

It can be shown that Eq.(B7) is only true if: (1) $\tilde{\hat{\boldsymbol{D}}}_{\mathrm{V}}^{\mathrm{II}} = \hat{\boldsymbol{D}}_{\mathrm{V}}^{\mathrm{II}}$, and (2) simple shear or irrotational deformations are considered. However, it can also be shown that Eq.(B7) cannot be generalised to other loading cases (e.g. where shear and uniaxial extension are superimposed), even if $\tilde{\hat{\boldsymbol{D}}}_{\mathrm{V}}^{\mathrm{II}} = \hat{\boldsymbol{D}}_{\mathrm{V}}^{\mathrm{II}}$. Hence, in general, case 2 is not identical to case 3 (and thus to approach I – case 1).

FIGURE CAPTIONS

Fig. 1. Simulation of uniaxial extension using different approaches and models; the applied nominal strain rate is 0.4 s^{-1}.

Fig. 2. Elongational viscosity predicted for uniaxial extension at various constant rates of elongation: $\eta_E = \{\sigma_{11} - \sigma_{22}\}\{1+e\}/\dot{e}$ where e is the applied nominal strain. Logarithmic scales.

Fig. 3. Simulation of start up of simple shear flow using different approaches and models; the applied shear rate is 0.4 s^{-1}.

Fig. 4. The first normal stress difference N_1 as predicted for start-up of simple shear flow at a shear rate of 0.4 s^{-1}.

Fig. 5. The second normal stress difference N_2 as predicted for start-up of simple shear flow at a shear rate of 0.4 s^{-1}.

Fig. 6. Shear viscosity predicted for start-up simple shear at various rates, $\eta_S = \sigma_{12}/\dot{\gamma}$ where $\dot{\gamma}$ is the shear rate. Logarithmic scales.

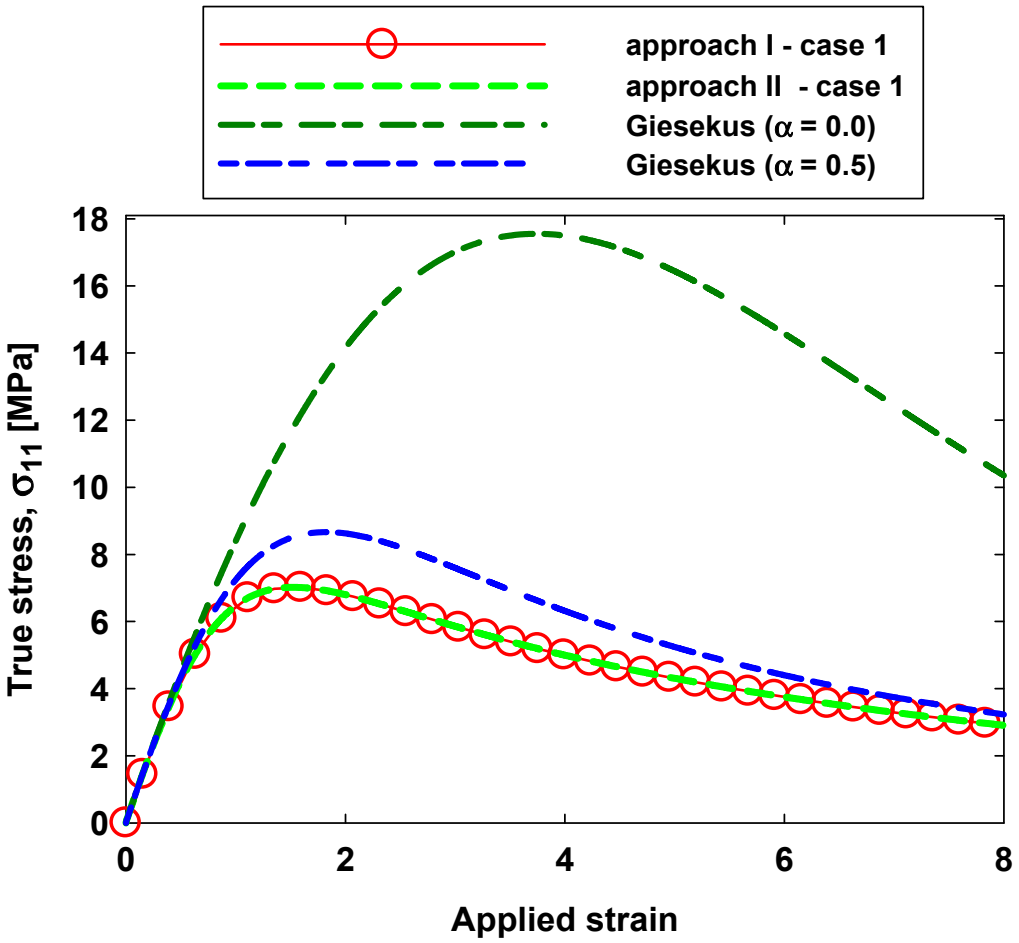

Fig. 1. Simulation of uniaxial extension using different approaches and models; the applied nominal strain rate is 0.4 s^{-1}.

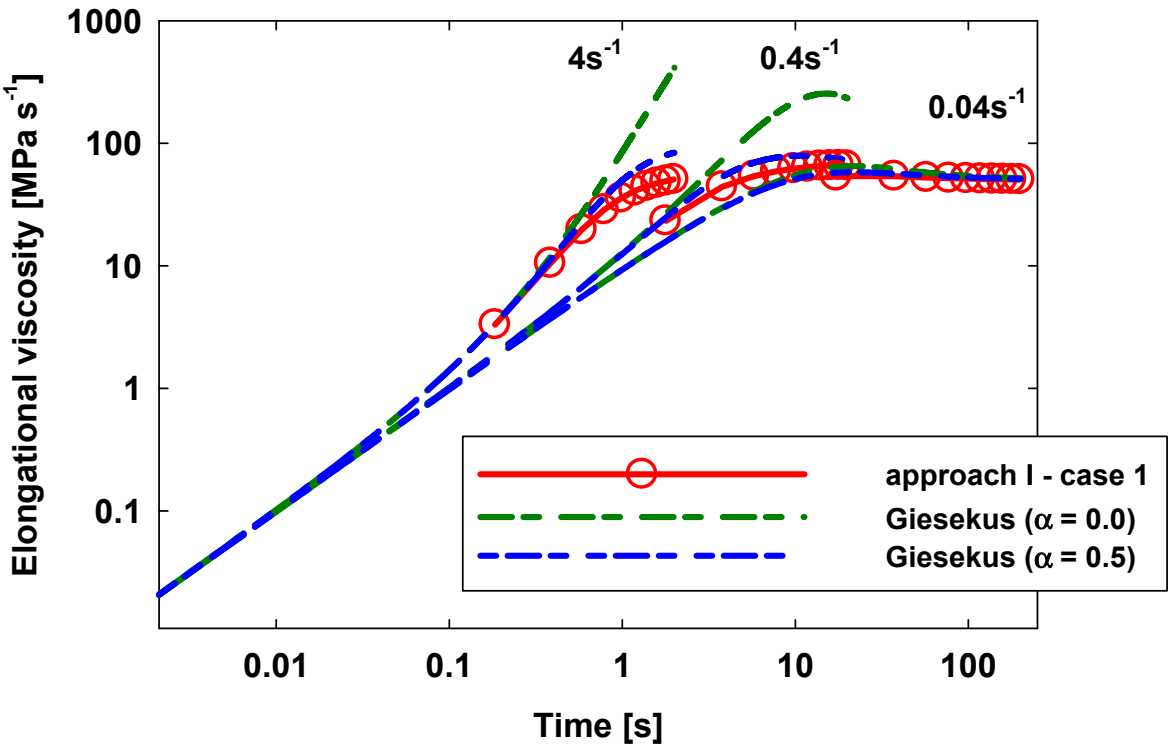

Fig. 2. Elongational viscosity predicted for uniaxial extension at various constant rates of elongation: $\eta_E = \{\sigma_{11} - \sigma_{22}\}\{1+e\}/\dot{e}$ where e is the applied nominal strain. Logarithmic scales.

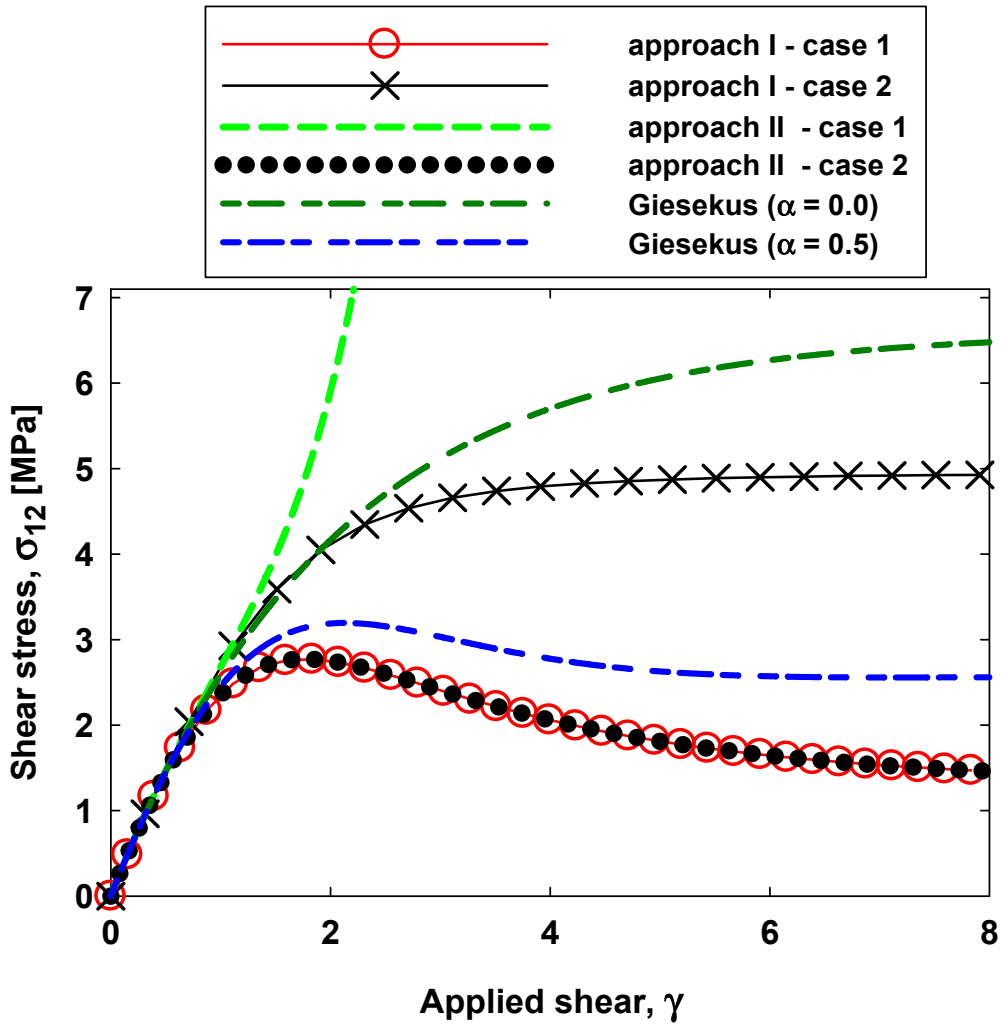

Fig. 3. Simulation of start up of simple shear flow using different approaches and models; the applied shear rate is 0.4 s^{-1}.

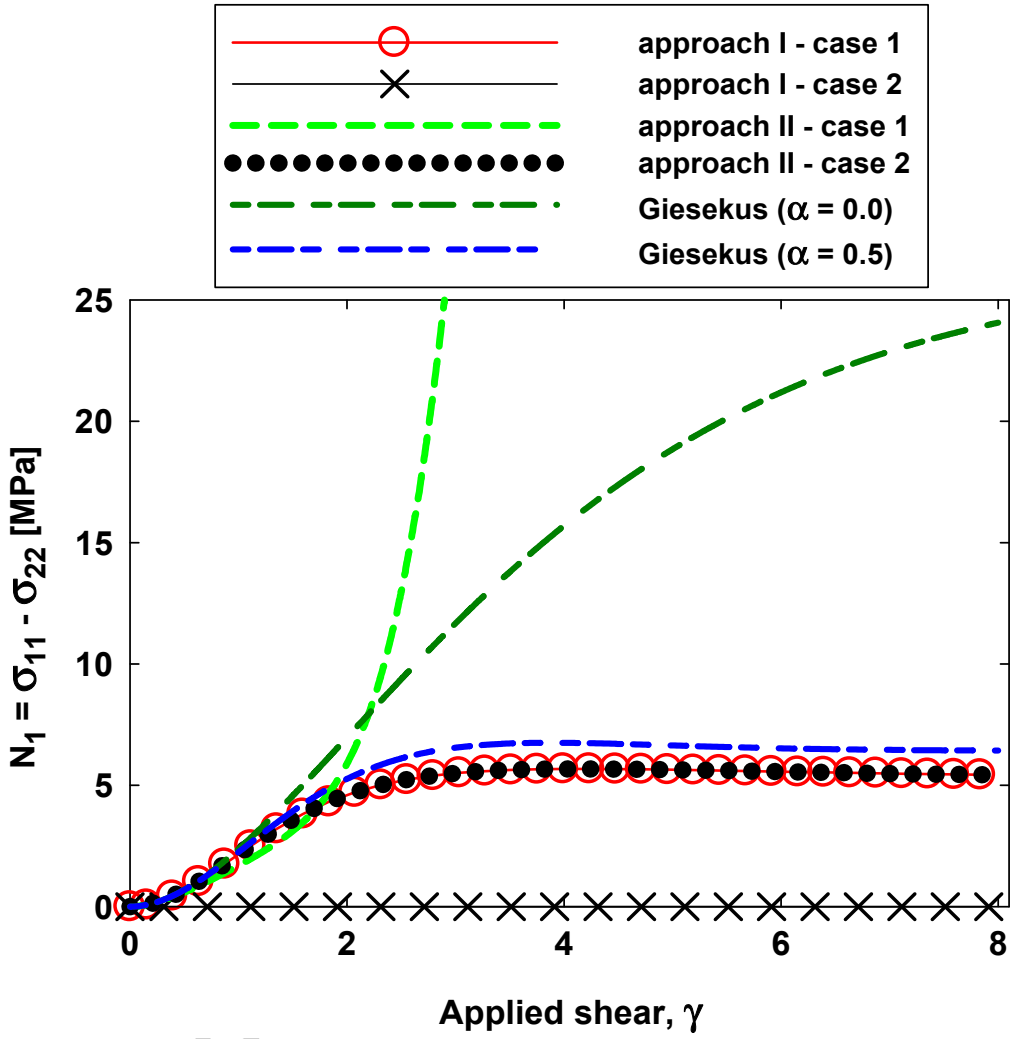

Fig. 4. The first normal stress difference N_1 as predicted for start-up of simple shear flow at a shear rate of 0.4 s^{-1}.

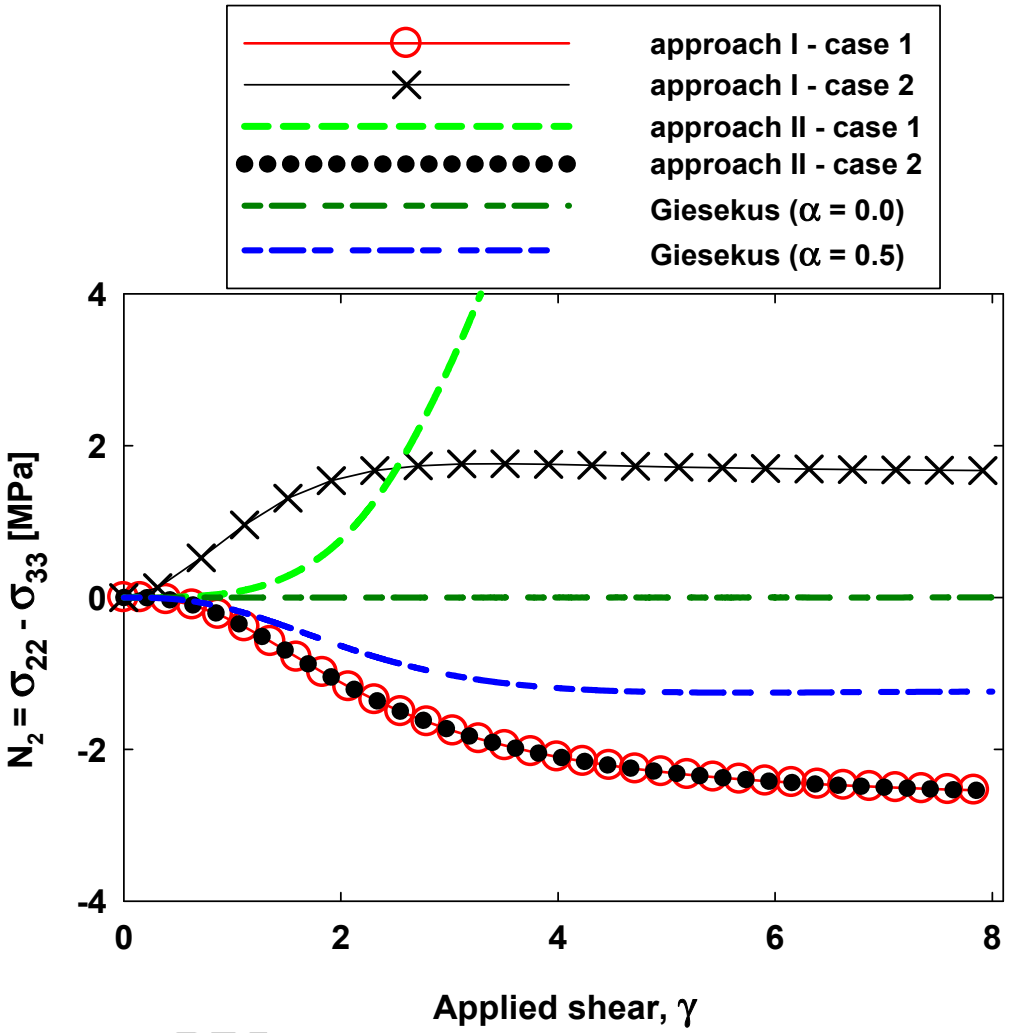

Fig. 5. The second normal stress difference N_2 as predicted for start-up of simple shear flow at a shear rate of 0.4 s^{-1}.

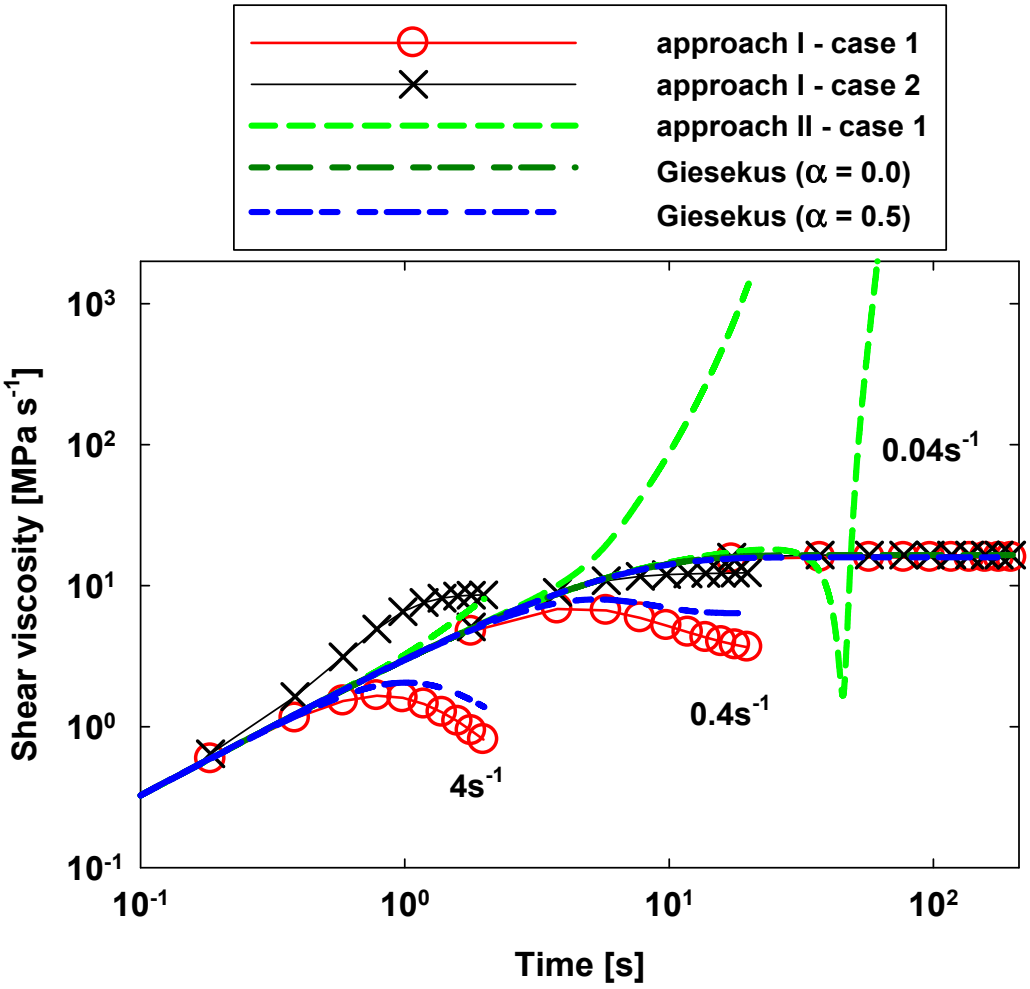

Fig. 6. Shear viscosity predicted for start-up simple shear at various rates, $\eta_S = \sigma_{12}/\dot{\gamma}$ where $\dot{\gamma}$ is the shear rate. Logarithmic scales.